

MEASUREMENT OF AIRFOIL HEAT TRANSFER
COEFFICIENTS ON A TURBINE STAGE*Robert P. Dring
Michael F. Blair
H. David JoslynUnited Technologies Research Center
East Hartford, Connecticut 06108

INTRODUCTION

The primary basis for heat transfer analysis of turbine airfoils is experimental data obtained in linear cascades. These data have been very valuable in identifying the major heat transfer and fluid flow features of a turbine airfoil. The question of major interest is how well all of these data translate to the rotating turbine stage. It is known from the work of Lokay and Trushin (Ref. 1) that average heat transfer coefficients on the rotor may be as much as 40 percent above the values measured on the same blades non-rotating. Recent work by Dunn and Holt (Ref. 2) supports the conclusion of Ref. 1. What is lacking is a set of data from a rotating system which is of sufficient detail as to make careful local comparisons between static cascade and rotor blade heat transfer. In addition, data is needed in a rotating system in which there is sufficient documentation of the flow field to support the computer analyses being developed today. Other important questions include the impact of both random and periodic unsteadiness on both the rotor and stator airfoil heat transfer. The random unsteadiness arises from stage inlet turbulence and wake generated turbulence and the periodic unsteadiness arises from blade passing effects. A final question is the influence, if any, of the first stator row and first stator inlet turbulence on the heat transfer of the second stator row after the flow has been passed through the rotor.

OBJECTIVES

The first program objective is to obtain a detailed set of heat transfer coefficients along the midspan of a stator and a rotor in a rotating turbine stage (Fig. 1). These data are to be such that the rotor data can be compared directly with data taken in a static cascade. The data are to be compared to some standard analysis of blade boundary layer heat transfer which is in use today. In addition to providing this all-important comparison between rotating and stationary data, this experiment should provide important insight to the more elaborate full three-dimensional programs being proposed for future research. A second program objective is to obtain a detailed set of heat transfer coefficients along the midspan of a stator located in the wake of an upstream turbine stage. Particular focus here is on the relative circumferential location of the first and second stators. Both program objectives will be carried out at two levels of inlet turbulence. The low level will be on the order of 1 percent while the high level will be on the order of 10 percent which is more typical of combustor exit turbulence intensity. The final program

*Work done under NASA Contract NAS3-23717.

objective is to improve the analytical capability to predict the experimental data.

PROGRESS

During the past year the following phases of the program were completed: (1) A turbulence generating grid was designed and installed in the turbine inlet which produced the target nominal value of 10% free-stream turbulence. (2) Aerodynamic documentation of the rotor and stator midspan surface pressure distributions was obtained. (3) Midspan heat transfer data were obtained on the rotor and stator for variations in inlet turbulence, rotor-stator axial spacing, and rotor incidence. Each of these three areas will now be discussed in greater detail.

1. Inlet Turbulence

As part of the present contract the effects of high levels of free-stream turbulence on the heat transfer distributions through the LSRR turbine blading will be examined. These heat transfer data will be obtained for a turbine inlet turbulence intensity of approximately 10 percent. This is typical of the level of turbulence measured at the exit of aircraft gas turbine combustors. For purposes of airfoil to airfoil consistency (circumferential uniformity) and so that the present results can be compared with other data on the effects of turbulence on heat transfer, the turbulence generated for these tests is required to be spatially uniform, nearly isotropic, and temporally steady (over time scales long when compared to the turbulent fluctuations). In addition the test turbulence must be generated in a manner such that there is a reasonably high intensity through the 1 1/2 stages of the turbine, i.e., the streamwise decay of the turbulence must be similar to that in an engine.

The turbulence generator selected consisted of a nearly square array lattice of three concentric rings spaced uniformly in the radial direction with 80 radial bars evenly spaced circumferentially. Both the rings and radial bars are of nearly square 1/2 inch cross-section. The mesh spacing of the bar is 2.1 inches radially and 4.5 degrees (2.1 in. at mid-annulus) circumferentially.

Preliminary indications are that without the grid installed the inlet turbulence was approximately 0.5% at an axial location 22% of axial chord ahead of the first stator leading edge. With the grid installed, at this same axial location, the inlet turbulence intensity was typically 9.8%. The spanwise distributions at four different circumferential locations (relative to the stator leading edge) are shown in Fig. 2. The data indicate that the turbulence is spatially uniform, nearly isotropic, and temporally steady.

2. Aerodynamics

The aerodynamic documentation of the turbine stage indicated that all parameters were very close to data obtained during prior testing with this turbine model. As an example, the stator and rotor pressure distributions are shown in Figs. 3a and 3b for the case with the small (15%) axial gap, design flow coefficient ($C_x/\bar{U}_m = 0.78$), and the inlet turbulence gener-

ating grid installed. Agreement with a potential two dimensional flow calculation at this midspan location is excellent. The computed surface velocity distributions are used as the input to the suction and pressure surface boundary layer calculations.

3. Heat Transfer

The method of fabrication of the heat transfer models was described in detail in the 1984 HOST review. Suffice it to say here that Joulean heating of a thin sheet of metal foil on the stator and rotor surfaces produces a nearly uniform surface heat flux. Conduction and radiation effects produce small departures from complete uniformity. Local airfoil surface temperatures are measured using thermocouples welded to the back of the foil and the air temperature is measured using thermocouples in the air stream. The secondary junctions to copper wire are all made on Uniform Temperature Reference blocks (Kaye Instruments, UTR-48N) and the data were recorded using a Hewlett-Packard 300 channel data acquisition unit (3497A/3498A), and an ice point reference (Kaye Instruments, K140-4). A 212 ring slip-ring unit (Wenden Co.) was used to bring heater power onto the rotor and to bring out the thermocouple data.

A low speed unheated test run indicated a max-to-min variation in absolute temperature for all thermocouples in all airfoils (rotor and stator, suction and pressure surfaces) of $\pm 0.3^{\circ}\text{F}$. As part of the procedure of taking the model data the temperature of the flow just upstream of the grid location was monitored at eight equally spaced circumferential locations. For these initial test cases it was decided that data would be recorded only if the outside ambient (rig inlet) conditions were such that the inlet temperature was below 65°F and that the temperature range of the eight inlet thermocouples was within approximately $\pm 1^{\circ}\text{F}$. These criteria were intended to assure that there would be both an adequate temperature difference between the heated surfaces and the freestream and a uniform temperature approach flow for the stator and rotor models. Preliminary examination of these data indicates that there was excellent run-to-run and day-to-day repeatability of results for nominally identical test conditions.

A sample set of rotor heat transfer distributions is presented in Figure 4. These data were all obtained with an axial rotor-stator separation of 15% chord. Data are presented for cases both with and without the turbulence grid installed for three flow coefficients (C_x/U_m). Although the rotor inlet relative velocity (W_1) differed widely for these three flow coefficients ($W_1=91.4, 115.0$ and 163.3 ft/sec for $C_x/U_m=0.68, 0.78$ and 0.96 respectively) the rotor exit relative velocity was invariant at $W_2=176$ ft/sec. For ease of comparison the Stanton numbers of Figure 4 were computed using the nearly constant rotor exit conditions. Computation of predicted heat transfer distributions for these test cases was not completed at the time of submittal of this interim report so the data are simply connected with straight line segments.

The three sets of data in the lower portion of Figure 4 (open symbols) were obtained without the turbulence generating grid installed. A comparison of the relative levels of Stanton numbers for these three cases indicates that: (1) the heat transfer rates near the trailing edge of both the suction and pressure surfaces are independent of flow coefficient and (2) the peak stagnation region ($S=0$) heat transfer obeyed the classic cylinder leading edge correlation with St inversely proportional to the square root of the Reynolds number based on nose diameter and approach relative velocity. The most distinct difference between the three low turbulence heat transfer distributions resulted near $S \sim 1$ inch. As C_x/U_m increased, a region of very high local Stanton number resulted at this x_m location. The basic cause of this spike in heat transfer is the suction surface overspeed ($S \sim 3/4$ in.), the strength of which is a function of the flow coefficient. At $C_x/U_m = 0.68$ there is only a slight overspeed followed by a favorable pressure gradient to midchord while for $C_x/U_m = 0.96$ the suction surface overspeed location has by far the highest velocity on the airfoil and is followed by a very strong adverse pressure gradient. For $C_x/U_m = 0.96$ the boundary layer is apparently unable to negotiate the adverse pressure gradient, separates, passes through a very short transition and reattaches as a high-speed, fully-turbulent layer. For $C_x/U_m = 0.68$ the boundary layer seems to experience an extended transition length through the favorable pressure gradient to near midchord. A much subdued version of this same phenomenon can be seen on the pressure surface where the most severe overspeed ($S \sim -1/2$ inch) occurs for $C_x/U_m = 0.68$.

A general increase in the levels of heat transfer was observed for the three cases with enhanced free-stream turbulence (solid symbols). Two of the most extreme local effects were: (1) near the suction surface overspeed where the freestream turbulence has severely increased the heat transfer and (2) at $S \sim -2$ inches for $C_x/U_m = 0.96$ where the free-stream turbulence produced a much shorter transition length.

Off-midspan data (not shown here) over the aft portion of the suction surface indicate much higher Stanton numbers near the root and tip. These enhanced heat transfer levels were almost certainly a product of the passage and tip-leakage vortex systems. It is anticipated that the flow convergence associated with these same corner vortices will cause the measured mid-span trailing edge Stanton numbers to fall well below values predicted for 2-d flow.

REFERENCES

1. Lokay, V. I., and Trushin, V. A.: Heat Transfer from the Gas and Flow-Passage Elements of a Rotating Gas Turbine. Heat Transfer - Soviet Research, Vol. 2., No. 4, July 1970.
2. Dunn, M.G., and Holt, J.L.: The Turbine Stage Heat Flux Measurements. Paper No. 82-1289, AIAA/ASME 18th Joint Propulsion Conference, 21-23, June, 1982, Cleveland, Ohio.

TURBINE STAGE AT 15% AXIAL GAP

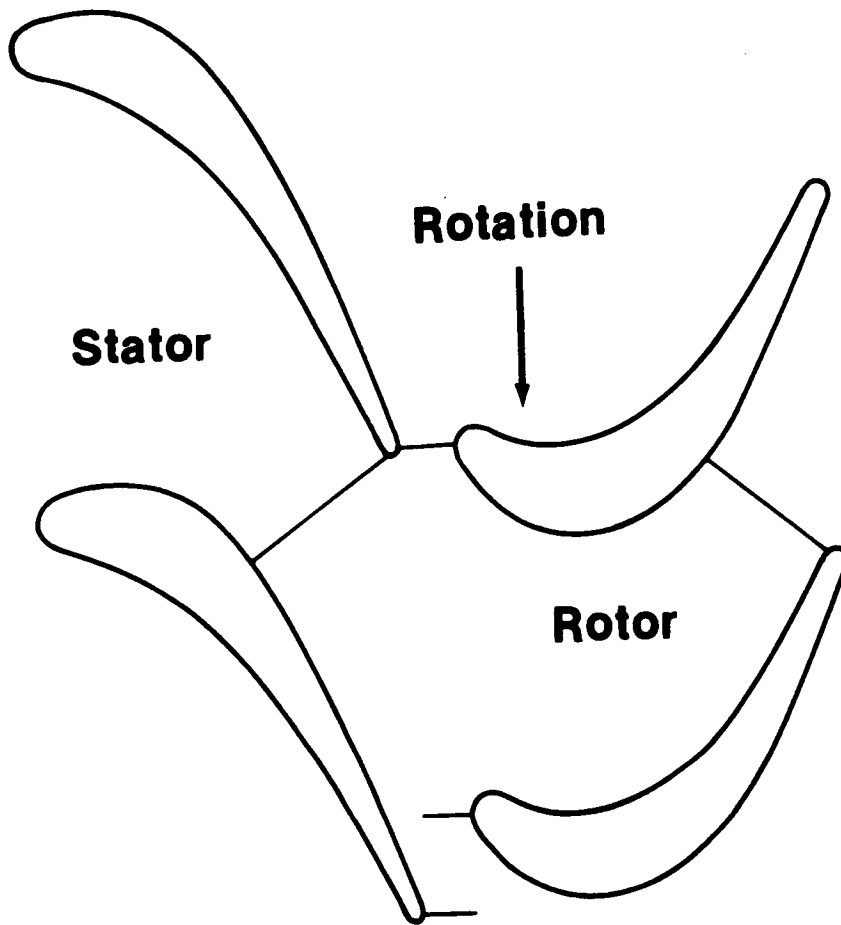


FIG. 1

STREAMWISE TURBULENCE (RMS)

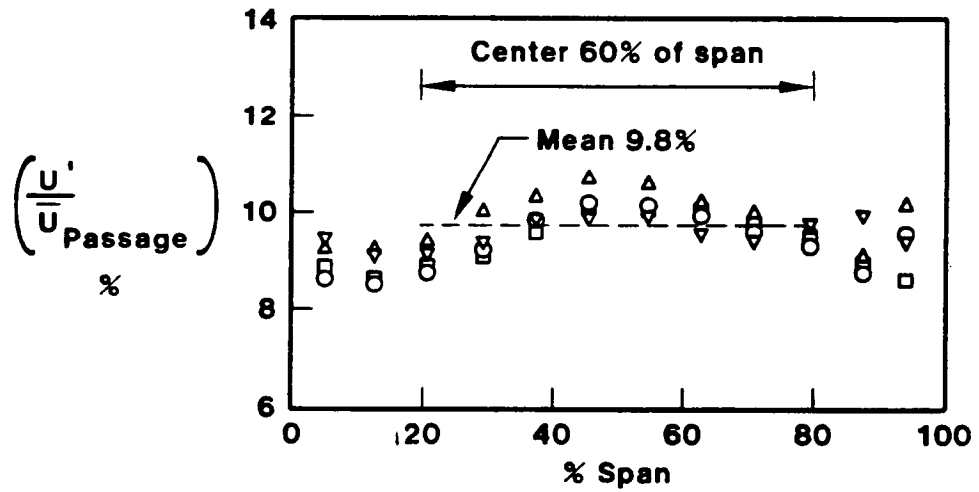


Figure 2

ORIGINAL PAGE IS
OF POOR QUALITY

FIRST STATOR PRESSURE DISTRIBUTION

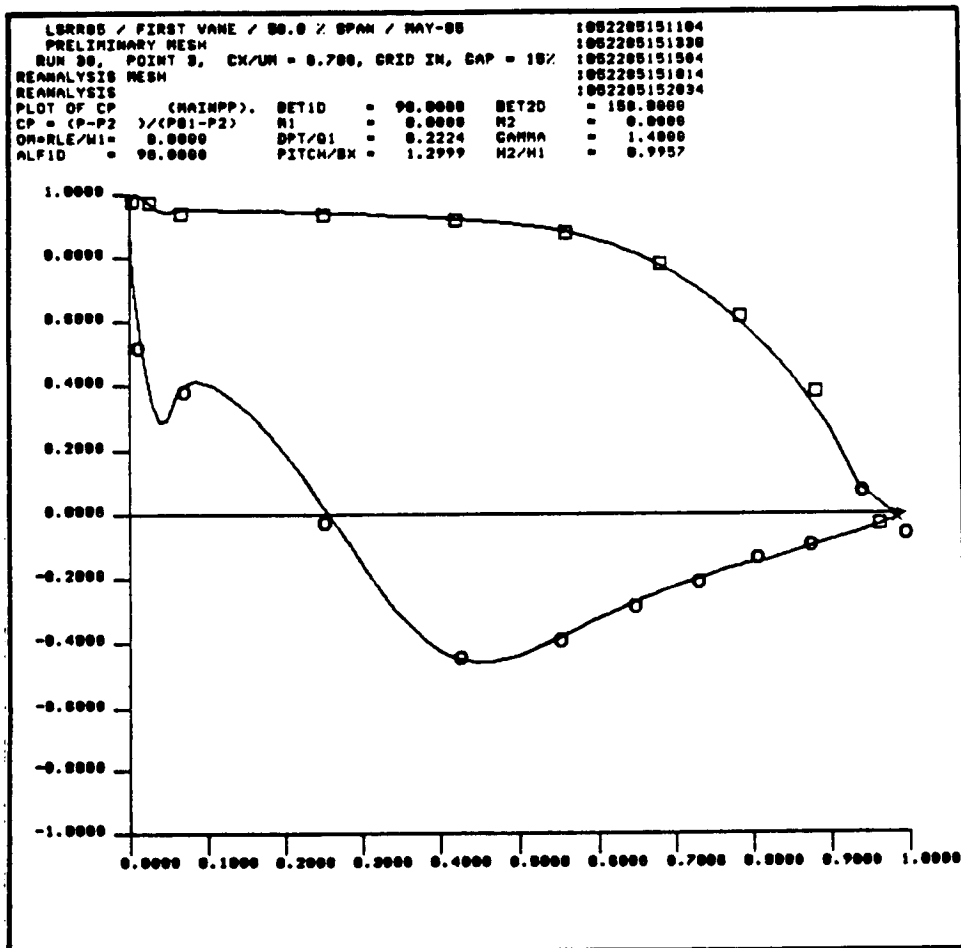


Figure 3a

ORIGINAL PAGE IS
OF POOR QUALITY

ROTOR PRESSURE DISTRIBUTION

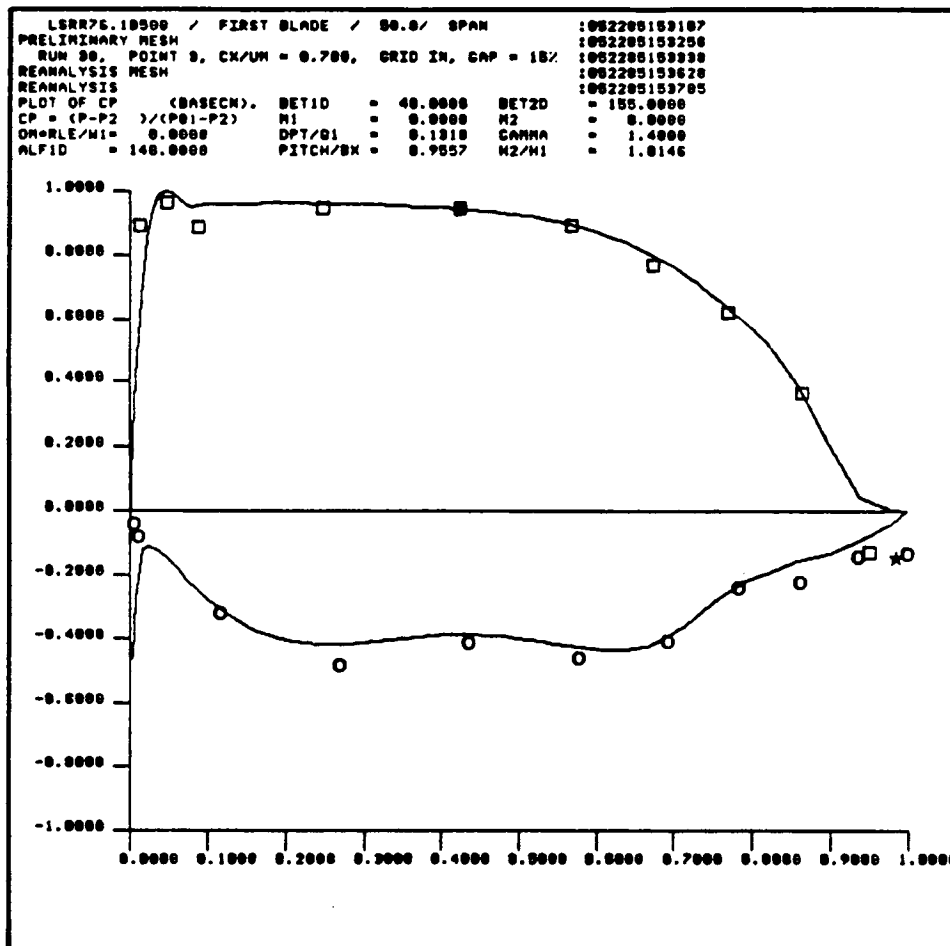


Figure 3b

ROTOR HEAT TRANSFER DISTRIBUTIONS

Close rotor-stator spacing

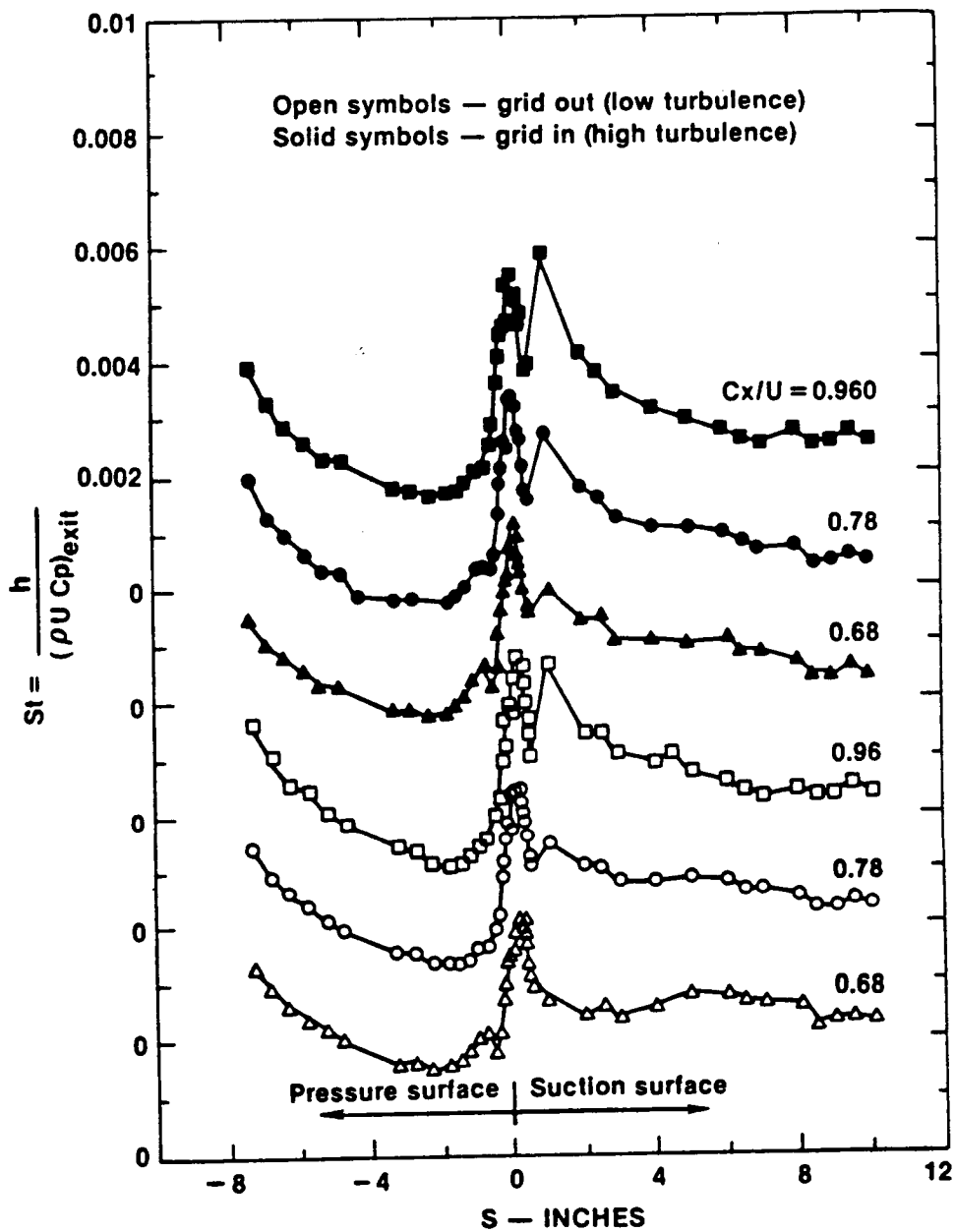


Figure 4